

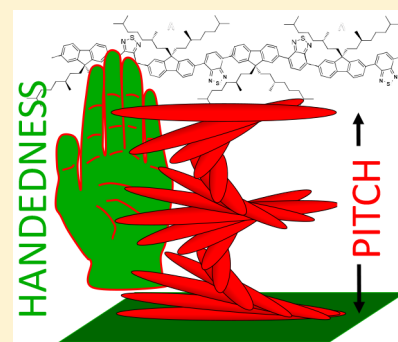
# Pitch and Handedness of the Cholesteric Order in Films of a Chiral Alternating Fluorene Copolymer

Chidambar Kulkarni,<sup>†</sup> Daniele Di Nuzzo,<sup>‡</sup> E.W. Meijer,<sup>†</sup> and Stefan C.J. Meskers<sup>\*,†</sup>

<sup>†</sup>Department of Chemical Engineering and Chemistry and Institute of Complex Molecular Systems, Eindhoven University of Technology, 5612 AZ Eindhoven, The Netherlands

<sup>‡</sup>Department of Physics, University of Cambridge, Cambridge CB2 1 TN, United Kingdom

**ABSTRACT:** The molecular organization in thermally annealed films of poly(9,9-bis((*S*)-3,7-dimethyloctyl)-2,7-fluorene-*alt*-benzothiadiazole) is investigated using polarized light. Measurement of linear polarization in transmission and reflection as a function of layer thickness and orientation directly show a left handed cholesteric organization with a pitch length of 600 nm. Results are corroborated by measurements of circularly polarized reflection and generalized ellipsometry and are compared to calculations of the optical properties based on the Maugin–Oseen–DeVries model. For wavelengths near the lowest allowed optical transition, light with the same handedness as the cholesteric arrangement (left) is found to be reflected and transmitted with a probability higher than right circularly polarized light. The high transmission for left polarized light is interpreted as an optical manifestation of the Borrmann effect.



## INTRODUCTION

$\Pi$ -conjugated molecular materials find application in optoelectronic devices, such as light emitting diodes and photovoltaic cells. The probability for optical transitions in these materials, which is an important factor controlling the efficiency in light emission and photovoltaic diodes, can in principle be influenced by the mesoscopic structure of the material. A periodic variation in the polarizability of the material with a typical length comparable to the wavelength of the optical transition of interest, changes the density of photon states and will affect the probability of spectroscopic transitions in a limited frequency range. In the extreme case, a photonic bandgap is established, i.e., in a certain frequency range practically all photon states are eliminated. The exclusion of photon states prohibits the absorption and/or emission of photons by the molecule in the material in the forbidden frequency range. A well-established route to create such a forbidden energy gap for photons in a particular direction is the introduction of chiral nematic order.<sup>1,2</sup> Photons with the same helicity as the molecular cholesteric arrangement are selectively reflected when their direction of propagation runs parallel to the axis of the cholesteric.

In this study we investigate thin layers (<400 nm) of an enantiomerically pure, chiral fluorene-based alternating copolymer,<sup>3,4</sup> poly(9,9-bis((*S*)-3,7-dimethyloctyl)-2,7-fluorene-*alt*-benzothiadiazole) **1**<sup>5–7</sup> ( $M_n$  ca. 5.5 kg/mol, PDI 2.20). This polymer shows liquid crystalline order at elevated temperature.<sup>8,9</sup> Upon rapid cooling, the molecular order in the liquid crystalline state is vitrified,<sup>10–12</sup> and at room temperature, chiral nematic order is evidenced by preferential reflection of left circularly polarized light.<sup>13</sup> Chiroptical properties of **1** and related polymers become very pronounced after thermal annealing in a liquid crystalline state, inducing long-range structural

order.<sup>14–17</sup> For films of polymer with thicknesses that are relevant for practical application in light emitting diodes or photovoltaic diodes, few methods exist to determine the pitch length of the cholesteric arrangement. The well-known Grandjean–Cano or wedge method does not work because of the high viscosity of the material. Second, because the films are relatively thin, no clear selective reflection band can be observed. Also optical rotation has been used to determine pitch length, because according to the De Vries theory, optical rotation should diverge for wavelengths approaching the selective reflection band. Since often the reflection band cannot be discerned, the viability of the De Vries description for optical rotation seems questionable. In this contribution we develop a novel method to determine pitch length in thin films based on linear dichroism in transmission and reflection, relying on the strong optical anisotropy of the individual polymer chains. This work extends the seminal contribution of Chen and co-workers,<sup>18</sup> who showed that polarized transmission measurements on a thin film of chiral fluorene nonamers provide information on handedness and pitch of the cholesteric molecular arrangement. Making use of this linear dichroism method, we determine the handedness and pitch of the cholesteric arrangement in a layer of chiral conjugated polymer. Complementary measurements on the circular polarization in reflection and optical rotation confirm the handedness. For aligned, thermally annealed films of **1** we find a pitch length of around 600 nm which is close to the wavelength of the lowest allowed absorption band in this material with an onset around 500 nm. For  $\pi$ -conjugated polymers, the contrast in

Received: October 16, 2017

Revised: December 3, 2017

Published: December 4, 2017

dielectric contrast in the direction parallel and perpendicular to the main chain is large for wavelengths near an optical resonance. Because the wavelength of the lowest allowed optical transition in the polymer **1** and its pitch length are comparable, many of the intriguing optical properties of cholesteric liquid crystals which are usually only observable in very thick films, now become apparent already in thin films.

## EXPERIMENTAL SECTION

**Synthesis.** Synthesis of **1** was carried out according to a previously reported procedure.<sup>7</sup> However, the crude product was purified according to reported procedures<sup>19,20</sup> to remove palladium(0) catalyst from the polymer.

Crude polymer was dissolved in chloroform (150 mL) and aq. ammonia solution (28–30%, 150 mL) was added and refluxed for 3 h followed by stirring at room temperature overnight.<sup>19</sup> The organic layer was separated using a separating funnel and to this was added ethylenediaminetetraacetic acid disodium salt dihydrate (2.1 g) and the solution was stirred overnight. The organic layer was extracted with water, washed with brine, dried over sodium sulfate, and evaporated under reduced pressure to about 10 mL. To this concentrated organic layer, a palladium scavenger, diethyldithiocarbamic acid diethylammonium salt (60 mg) was added and stirred under dark and argon atmosphere for 6 h.<sup>11</sup> Then the solution was poured onto cold methanol (300 mL) and the precipitate was collected by suction filtration and dried under vacuum at 60 °C overnight. The precipitate was further subjected to Soxhlet extraction with acetone to remove small oligomers. The insoluble precipitate was dissolved in minimum amount of THF and precipitated into cold methanol. The precipitate was filtered and dried under vacuum at 60 °C overnight to obtain a yellow powder.

**Gel Permeation Chromatography.** PS standard, THF; Apparent  $M_n$ : 5.54 kg mol<sup>-1</sup>,  $M_w$ : 12.24 kg mol<sup>-1</sup>, PDI ( $M_w/M_n$ ) = 2.20.

**Nuclear Magnetic Resonance.** <sup>1</sup>H- and <sup>13</sup>C spectra were in accordance with the previous reports.<sup>7</sup>

**Film Preparation.** A solution of **1** in 9:1 (v/v) chloroform:chlorobenzene was heated in an oil bath at 70 °C for 2 h and then within an hour was spin-coated (2000 rpm, 60 s, maximum acceleration) on clean glass slides and rubbed polyimide coated glass slides. The glass slides were annealed at 150 °C for 15 min under nitrogen atmosphere (glovebox).<sup>5,21</sup> To obtain films of different thickness, concentration of **1** was varied from 5 mg/mL to 50 mg/mL. Film thickness at each concentration (5, 7.5, 15, 30, and 50 mg/mL) of **1** was determined for films on clean glass slides using Dektak 150 Surface Profiler and a similar thickness was assumed on rubbed polyimide coated glass slides as well.

**Polyimide Alignment Layer.** 2.5 cm × 2.5 cm glass slides were cleaned by sonication for 10 min each with acetone and isopropyl alcohol. The glass slides were then etched in a UV-ozone photoreactor (PR-100) for 30 min. Polyimide (AL 1051) was spin-coated on etched glass-slides (5000 rpm, 40 s, 500 rpm acceleration) and then annealed at 180 °C for 90 min. The polyimide facing side was rubbed on a velvet cloth to induce planar alignment.

**Polarized Reflection and Transmission Measurement.** Polarized reflection and transmission measurement were performed using a Woollam WVASE ellipsometer using the general Mueller matrix measurement protocol. Reflection measurement under normal incidence with selection of the reflected intensity, were done used a home-built setup described earlier.<sup>13,22</sup>

## RESULTS AND DISCUSSION

In Figure 1 we show polarized transmission spectra for a thermally annealed film of **1** with a thickness of  $d = 24$  nm on a

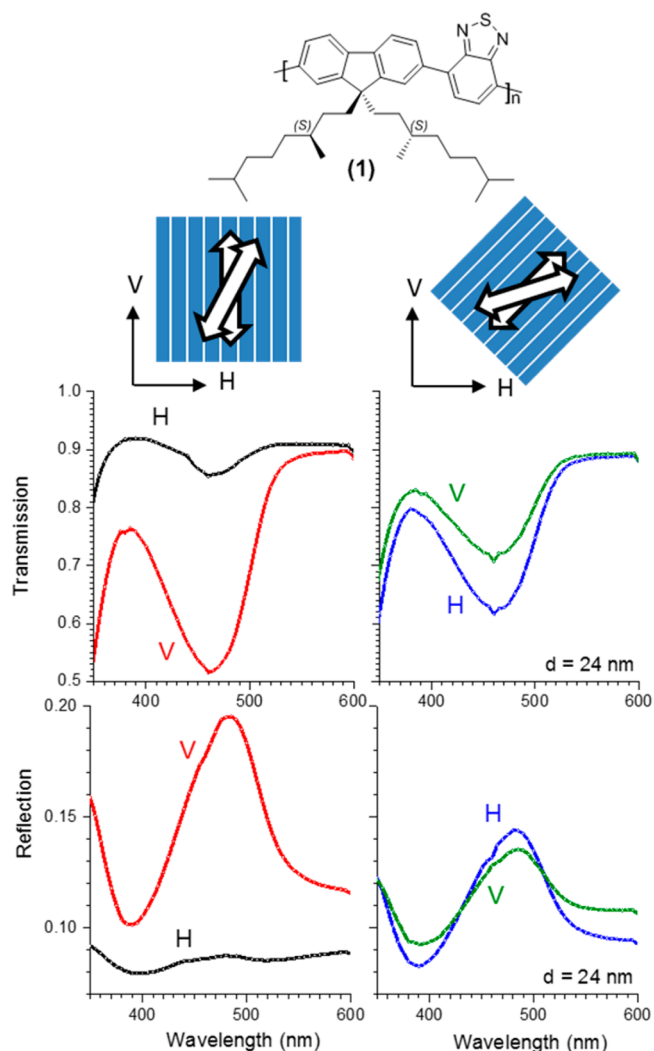


**Figure 1.** (Top) Chemical structure of the polymer **1**. (Middle) Schematic of the direction of the polyimide alignment layer and the orientation of the transition dipole moments of the  $\pi$ -conjugated polymer chains in a thin film of annealed polymer. (Bottom) linear dichroism in transmission and reflection for thermally annealed film of **1** on rubbed polyimide with the rubbing direction vertical (left) and rotated over +45° (right) as seen from the light source with the layer of conjugated polymer directly facing the viewer. Thickness of the layer of **1**:  $d = 24$  nm.

rubbed polyimide substrate. Transmission spectra for two different orientations of the polymer film are shown: one with the rubbing direction of the underlying alignment layer in the vertical direction and the other with rubbing direction rotated clockwise over +45° with the vertical as seen from the light source directly facing the polymer layer. The minimum in transmission near 460 nm corresponds to electronic excitation of the polymer chain via the allowed  $S_1 \leftarrow S_0$  electronic transition. This transition is of  $\pi-\pi^*$  orbital nature and polarized in a direction along the polymer backbone.<sup>23</sup> As expected for the vertically oriented polymer film, the transmission of light resonant with the electronic transition, shows strong linear dichroism with vertically polarized (V) incident light being

transmitted with far lower probability that horizontally polarized (H) incident light. The dichroism is consistent with alignment of the polymer chains in the direction of rubbing in the polyimide orientation layer. Also the reflection of the vertically oriented film is strongly polarized in the vertical direction. If we rotate the film over  $+45^\circ$ , the dichroism for V and H polarized light in reflection and transmission is strongly reduced. Yet we notice that for the  $+45^\circ$  orientation, H polarized light is transmitted with lower probability than V. In reflection, H is reflected more strongly than V for light at resonance with the  $S_1 \leftarrow S_0$  transition. This shows that in the film oriented  $+45^\circ$ , the orientation of the chains is biased toward the H direction. This bias can be accounted for by assuming a left-handed cholesteric arrangement of polymer chains.

In Figure 2, we summarize linearly polarized transmission and reflection measurements as shown in Figure 1 for films of **1** with various thickness. First we calculate the maximum extinction ( $E = -^{10}\log T$ ) for the  $S_1 \leftarrow S_0$  band and then compute the degree of linear polarization for V and H polarizations according to

$$p_E^{VH} = \frac{E_V - E_H}{E_V + E_H} \quad (1)$$

The degree of polarization for the films with vertical and with  $+45^\circ$  orientation are shown in the top part of Figure 2. Clearly for the thinnest films the degree of polarization is the largest. As the film thickness increases a damped oscillatory pattern emerges. In order to account for the measurements we assume simplistically that the extinction in, say, the V direction is proportional to the square of the component of the transition dipole moment integrated over the entire thickness of the film:

$$\begin{aligned} E_V(d, \chi) &\propto \int_0^{2\pi d/\text{pitch}} \cos^2(\phi + \chi) d\phi \\ E_H(d, \chi) &\propto \int_0^{2\pi d/\text{pitch}} \sin^2(\phi + \chi) d\phi \end{aligned} \quad (2)$$

with  $d$  the thickness of the film,  $\phi$  the angle between the vertical direction and the local director of the polymer chains film and  $\chi$  the angle describing the orientation of the film with  $\chi = 0^\circ$  referring the rubbing direction parallel to V. In eq 2 the integration ranges from zero to  $\phi_{\text{top}}$ , i.e., the angle between the director of the cholesteric at the top surface of the film and the direction of rubbing of the underlying substrate:

$$\phi_{\text{top}} = 2\pi \frac{d}{\text{pitch}} \quad (3)$$

Good agreement between experimental data and predictions from eq 2 can be obtained assuming a left-handed cholesteric order with a pitch length of 600 nm. To illustrate this we note that for films with 300 nm thickness the director of the cholesteric arrangement, makes exactly half a turn when going from the bottom to the top surface of the film. As a consequence of this half turn, the dichroism in extinction vanishes for all orientations of the film, consistent with the experiment.

For the linear polarization in reflection  $R$  by the films of **1**, an analysis similar to the one described above applies. We first introduce the degree of polarization in reflection

$$p_R^{VH} = \frac{R_V - R_H}{R_V + R_H} \quad (4)$$

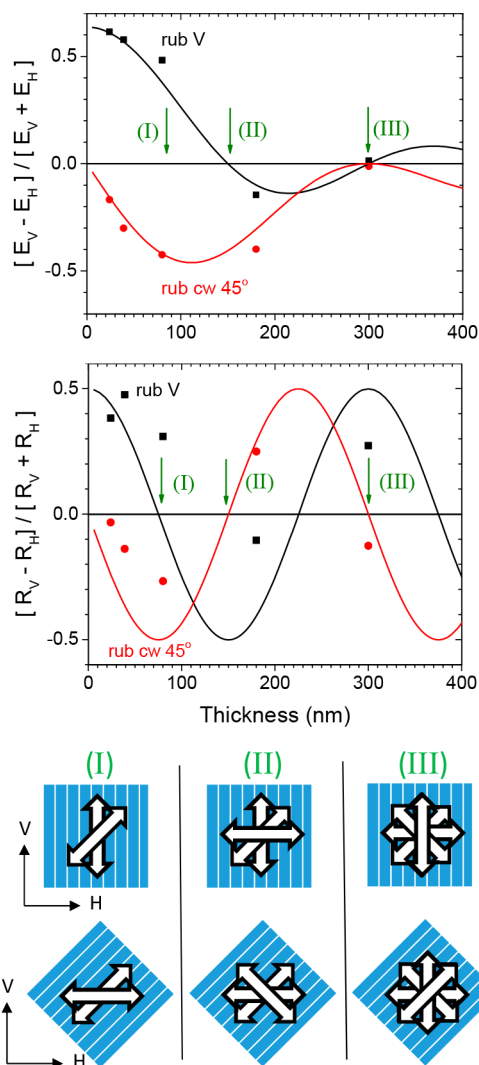


**Figure 2.** (Top) Degree of linear polarization in the extinction of vertically and horizontally polarized light through annealed and aligned films of **1** for orientations with rubbing direction vertical (black line) and rotated  $+45^\circ$  (red line) with respect to the vertical direction as seen from the source with the layer of **1** directly facing the source. Lines show a fit to the data of eq 2 with pitch = 600 nm. (Middle) Corresponding degree of polarization in reflection measured at  $15^\circ$  angle of incidence. Lines show a fit to the data of eq 4 with pitch = 600 nm. (Bottom) Schematic of the left handed cholesteric arrangement of polymer chains on the alignment layer for three characteristic thicknesses.

Next, we assume that the linear polarization in reflection is determined by the orientation of the polymer chains at the top surface of the polymer film facing the light source.

$$\begin{aligned} R_V(d, \chi) &\propto \cos^2\left(\frac{2\pi d}{\text{pitch}} + \chi\right) \\ R_H(d, \chi) &\propto \sin^2\left(\frac{2\pi d}{\text{pitch}} + \chi\right) \end{aligned} \quad (5)$$

Assuming a pitch length of 600 nm and a left-handed arrangement, the dependence of the degree of polarization in reflection on film thickness can quantitatively be accounted for (see Figure 2 middle).

An objection that may be raised to the above treatment of especially the linearly polarized reflection data, is that due to the

left-handed helical arrangement with pitch length close to the wavelength of observation, the reflection should be mainly circularly polarized. In order to investigate the light reflection in more detail, we have resorted to reflection measurements under exactly normal incidence in which not only the polarization of the incoming light but also the polarization of the reflected light can be selected, see Figure 3.

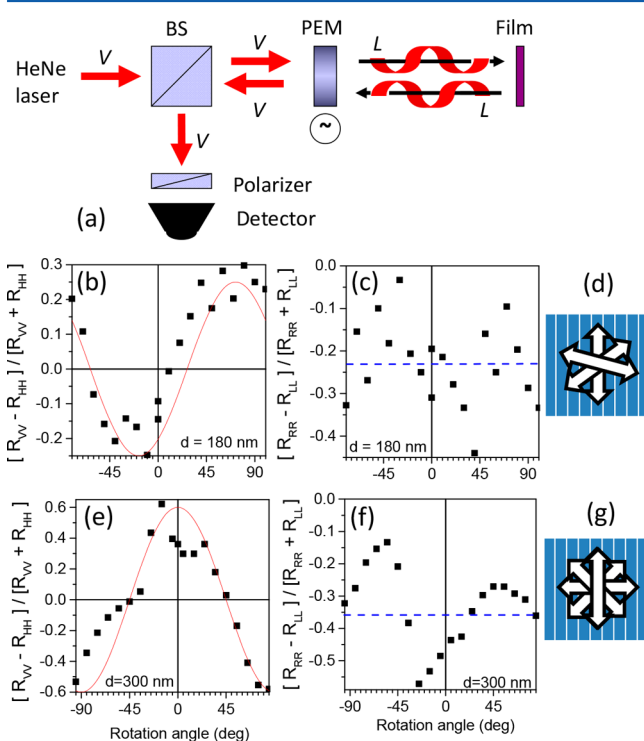


**Figure 3.** (a) Schematic of the experimental set up for measurement of reflection from a film under normal incidence with selection of both the incoming and reflected polarization. V vertically linear polarized light, BS beam splitter, PEM photoelastic modulator. The case of the modulator at quarter wavelength retardation is shown with left circularly polarized incident light reflected as left circular polarized light by the cholesteric film. (b) Degree of linear polarization in reflection for vertically polarized (V) incident light into V reflected light and horizontally polarized (H) incident light into H reflected light for an aligned film of **1** with thickness  $d = 180$  nm as a function of the rotation angle of the film around the surface normal. Zero rotation refers to the rubbing direction being vertical. Positive rotation refers to turning the polymer film in the clockwise direction as seen from the light source facing the polymer on top of the rubbed substrate. Wavelength of light: 543 nm. Red curve eq 7 with  $d = 300$  nm and pitch = 600 nm, (c) degree of circular polarization for right circularly polarized (R) incident light into R reflected light and left circularly polarized (L) incident light into L reflected light. Dashed blue line shows the average degree of circular polarization (c) schematic of the director in the 180 nm thick cholesteric film with a pitch of 600 nm. (e, f, and g) Similar for a 300 nm thick film of **1**.

From measurements of the reflection with vertical polarization of incident and reflected light and the corresponding measurement with horizontal incoming and outgoing polarization we calculate the degree of polarization in reflection according to

$$p_R^{VVHH} = \frac{R_{VV} - R_{HH}}{R_{VV} + R_{HH}} \quad (6)$$

This degree of polarization has been measured for a large number of different orientations of the polymer film by rotation

the film around its surface normal. In Figure 3 the dependence of the polarization on orientation is shown for the two thickest aligned films studied. Using eq 5 and simplifying the denominator in (eq 6) to unity, we expect:

$$p_R^{VVHH}(\chi) \propto \left( \cos^2 \left( \frac{2\pi d}{\text{pitch}} + \chi \right) - \sin^2 \left( \frac{2\pi d}{\text{pitch}} + \chi \right) \right) \quad (7)$$

The relationship (eq 7) is illustrated in the left part of Figure 3 for pitch length  $d = 600$  nm.

Interestingly, the experimental setup illustrated in Figure 3 can also be used to measure the reflection of left circularly (L) polarized light reflected as L and right circularly polarized light reflected as R. This type of reflection is characteristic for cholesteric liquid crystals. In contrast, reflection of circularly polarized light at dielectric interface occurs with inversion of circular polarization. We define a degree of polarization for this type of cholesteric reflection:

$$p_R^{RLL} = \frac{R_{RR} - R_{LL}}{R_{RR} + R_{LL}} \quad (8)$$

Results for the cholesteric circularly polarized reflection are shown in the left part of Figure 3. We find that cholesteric reflection of left circular polarized is more efficient than the corresponding reflection of right circular polarization. Because cholesteric liquid crystals selectively reflect light with the same helicity as their cholesteric ordering, these measurements support the conclusion of a left-handed organization in the films of **1**. The variation of the degree of circular polarization in the reflection with the orientation of the film which can be observed for the film with 300 nm thickness (Figure 3c) is currently not understood and may indicate that the reflected light may actually be polarized elliptically rather than circularly. In summary, by controlling also the polarization of the light detected in the reflection, we find that both linear and circular polarization measurements confirm a left-handed molecular organization in films of **1**.

Having now established a firm basis for the assignment of a left-handed cholesteric arrangement, the question arises naturally whether any circular selective reflection bands arise. It is well-known that in thick films of cholesteric liquid crystals of at least several microns, spectrally quite narrow selective reflection bands occur. In thinner films, however, the width of these reflection bands broaden.<sup>1</sup> In Figure 4 we present spectrally resolved circular selective reflection measurements on aligned films of **1**. These selectivities can be extracted out of the so-called Mueller matrix obtained from generalized ellipsometric measurements. In these experiments the angle of incidence is  $15^\circ$  and the polarization of the incident light is controlled and the total (unpolarized) reflected intensity is recorded.

In the left part of Figure 4 we show the degree of circular polarization in reflection obtained as the 1,4 element of the Mueller matrix, defined according to

$$p_R^{RL} = \frac{R_R - R_L}{R_R + R_L} \quad (9)$$

As can be seen, even the thinnest films show preferential reflection of left circularly polarized light for wavelengths exceeding the wavelength of maximum absorption for the  $S_1 \leftarrow S_0$  transition. The degree of polarization in these thin films is however quite low. For the two thickest films, circular selective reflection is more pronounced and the typical undulatory pattern

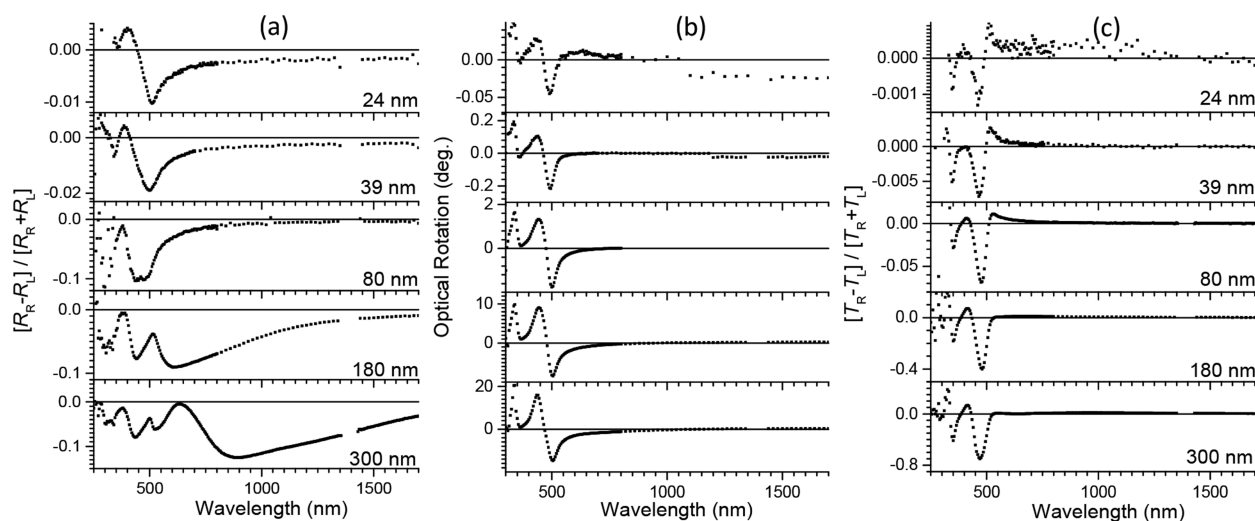


**Figure 4.** (a) Degree of circular polarization in reflection  $R$  of light by aligned films of **1** for various thicknesses of the cholesteric layer in the range 24–300 nm. Angle of incidence:  $15^\circ$ . (b) Optical rotation of plane polarized light upon transmission through the film under incidence along the surface normal, averaged over two orientations of the polymer films ( $0^\circ$  and  $45^\circ$ ). (c) Degree of circular polarization in transmission  $T$  of light incident along the surface normal.

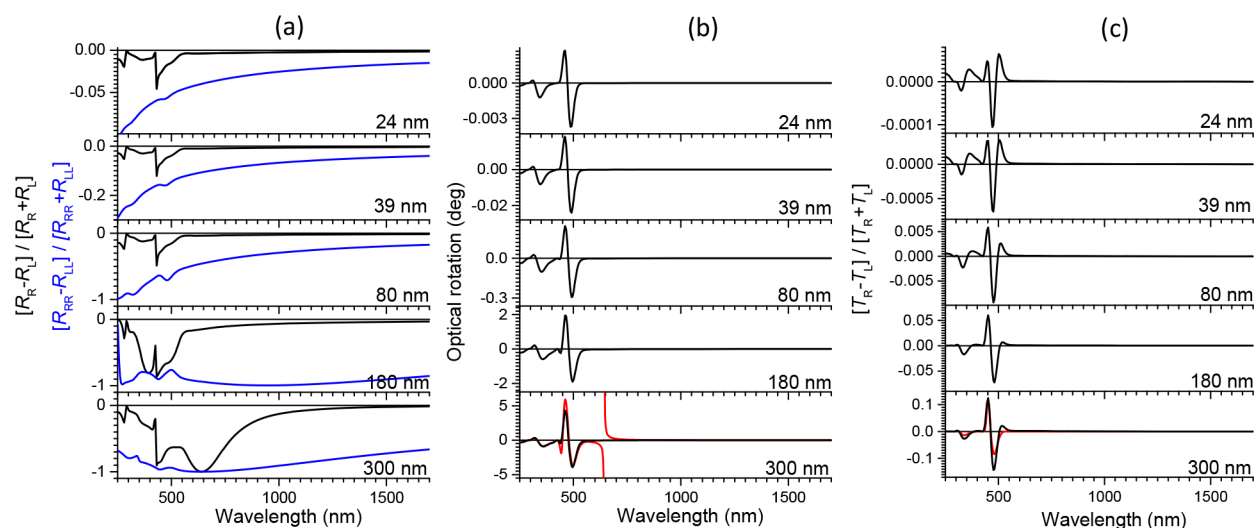


**Figure 5.** Theoretical predictions for the Maugin–Oseen–DeVries model based on the exact solutions as described by Good and Karali. (a) Degree of circular polarization in reflection  $p_R^{RL}$  (black line) and  $p_R^{RRL}$  (blue line). (b) Black line: Optical rotation of plane polarized light upon transmission through the film under incidence along the surface normal, averaged over two orientations of the polymer films ( $0^\circ$  and  $45^\circ$ ). Red line in the lowest panel: prediction from real part of eq 10. (c) Black line: Degree of circular polarization in transmission. Normal incidence. Red line in lowest panel: Prediction from imaginary part of eq 10.

of the circular polarization expected for thin cholesteric films is indeed observed.

The handedness and pitch lengths for cholesteric materials have previously also been estimated from study of the optical rotation and circular dichroism.<sup>24–26</sup> We now also apply these methods to the films of **1**. In Figure 4b, the rotation of plane of linearly polarized light upon transmission through films of **1** under normal incidence is shown. The optical rotation shown is an average over two orientation of the film (rubbing direction vertical and at  $+45^\circ$ ) and has been obtained from the Mueller matrix for transmission. The sign of the optical rotation is according to the convention in chemistry. All film studied show negative optical rotation for wavelengths near 500 nm. Curiously, the optical rotation spectra show no specific feature in the wavelength region matching the pitch of the cholesteric arrangement.

The optical rotation  $\phi$  of cholesteric liquid crystal is usually interpreted in terms of the De Vries equation. The De Vries equation for the specific rotation reads:<sup>1</sup>

$$\frac{\phi}{d} = P \frac{k_1^4}{8q_0(k_0^2 - q_0^2)} \quad (10)$$

with

$$k_0^2 = \left( \frac{2\pi}{\lambda_{\text{vac}}} \right)^2 \left( \frac{\epsilon_{\parallel} + \epsilon_{\perp}}{2} \right) \quad (11)$$

$$k_1^2 = \left( \frac{2\pi}{\lambda_{\text{vac}}} \right)^2 \left( \frac{\epsilon_{\parallel} - \epsilon_{\perp}}{2} \right) \quad (12)$$

and  $q_0 = 2\pi/\text{pitch}$ . Eq 10 is an approximate solution to the wave equation for electromagnetic waves traveling along the helical axis in the Maugin–Oseen–DeVries model for a cholesteric.<sup>27–29</sup> Interestingly the DeVries equation predicts a discontinuity at the wavelength of the electromagnetic waves inside the medium that matches the pitch of the chiral nematic. This discontinuity is illustrated in Figure 5b by the red line.

The discontinuity in the optical rotation predicted by eq 10 is not observed in our experiment. In fact this discontinuity also does not occur in the exact solution of wave equation for electromagnetic waves as given by Belyakov<sup>30</sup> and Good and Karali.<sup>31</sup> In Figure 5 we illustrate these exact solutions computed using an adaptation of the method described by Good and Karali. In the calculations we use complex dielectric functions determined experimentally from ellipsometry on thin annealed and unaligned films of 1. Comparing Figures 5 and 4, we notice that the calculated reflection and optical rotation are in qualitative agreement. The calculations correctly predict strong thickness dependence of the selective reflectivity and the optical rotation. The optical rotation according to the exact solution matches very closely the prediction from the DeVries eq 10, except for the discontinuity at the wavelength matching the pitch of the medium. Calculations using the Good and Karali formalism for films with thickness in the range of several microns, show features that start to resemble the discontinuity in optical rotation predicted by eq 10. We conclude that the DeVries equation does not correctly predict the optical rotation for thin films in the wavelength range corresponding to the pitch length.<sup>32</sup>

Finally we focus on the circular differential transmission of light through aligned films of 1. In Figure 4c the degree of circular polarization in the transmission of light is shown, defined according:

$$p_T^{\text{RL}} = \frac{T_R - T_L}{T_R + T_L} \quad (13)$$

Reasons for studying transmission rather than the more commonly used circular differential absorption also known as circular dichroism are the following. Because of the selective reflection and scattering of light by the aligned cholesteric material, determining true absorption and the associated circular differential is complicated and involves combination of several spectroscopic observables. Circular differential transmission is well-defined and can be measured directly. The second reason is a practical one. Commercial circular dichroism spectrometers are designed, optimized and calibrated to detect very small circular dichroism signals. The differentials for the materials under study can, however, be extremely large and partially fall outside the usual measurement range of the commercial spectrometers. The degree of polarization in (eq 13) equals the 1,4 element of the normalized Mueller matrix in generalized ellipsometry and the sign of (eq 13) is consistent with the sign of the dissymmetry ratio used in circular dichroism spectroscopy ( $g_{\text{abs}} = 2(A_L - A_R)/(A_L + A_R)$  with  $A$  the absorbance).

As can be seen in Figure 4c, the aligned films of 1 all show a negative degree of polarization for wavelengths near the maximum in the  $S_1 \leftarrow S_0$  transitions. The degree of polarization increases rapidly with film thickness. For the thickest film (300 nm), the value for  $p_T^{\text{RL}} = -0.8$  is close to the theoretical limit for fully selective transmission of left polarized light,  $p = -1$ . The  $p$  value for wavelengths just below the lowest allowed transition is positive, which can be attributed to selective reflection.

Up to now, we have interpreted chiroptical properties of films of 1 in terms of their mesoscopic chiral nematic molecular organization.<sup>33–35</sup> In principle, however, also the helicity of individual polymer chains could contribute to the circular differential signals.<sup>36</sup> In the latter case, because the chiroptical effects arise from the intramolecular organization, one expects the degree of circular polarization and the specific optical rotation are independent of the thickness of this film. Indeed from molecular chiroptical spectroscopy on dilute solutions, the dissymmetry ratio and specific optical rotation are known to be intrinsic properties of the individual molecules. In Figure 6 we

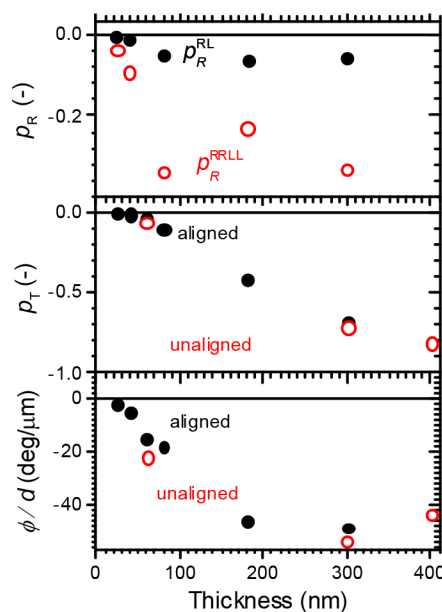


**Figure 6.** Degrees of polarization  $p$  in reflection (a) and transmission (b) according to eqs 4, 6, and 13 as a function of film thickness for 1. (c) Specific optical rotation of films of 1. In (b) and (c) also results for unaligned, annealed films of 1 are shown as open red symbols.

have summarized the maxima of the various degrees of circular polarization as well as the specific optical rotation for films with different thickness. As can be seen, all these chiroptical properties show a strong variation with the thickness of the film. These dependencies, which are in qualitative agreement with the predictions for the Maugin–Oseen–DeVries model see Figure 5, indicate that contributions to the chiroptical properties under study arising from the intrinsic chiral molecular structure are negligibly small.

For wavelengths near the allowed  $S_1 \leftarrow S_0$  transition we find that, left circularly polarized light is both reflected and transmitted with a higher probability than right circularly polarized light. This implies that the right circularly polarized light must be absorbed more strongly than left. In contrast, linearly polarized light with polarization parallel to the direction of the main chain of the conjugated polymers is reflected with higher probability than the orthogonal polarization but transmitted with lower probability by thin films, see Figure 1. The peculiar anomalous behavior of the circular polarizations may be interpreted as an optical manifestation of the Borrmann effect.<sup>37,38</sup> The latter effect is known from X-ray spectroscopy and describes an anomalously low absorption of X-rays in thick crystals when the crystal is set for a Bragg reflection. In absorbing cholesteric liquid crystals a related optical effect is known, where upon addition of an infrared absorbing dopant, the circular

polarization which is reflected with the highest probability in the absence of dopant acquires the highest transmission coefficient after addition of the absorbing species.<sup>39,40</sup>

## CONCLUSION

The optical properties of thin films of the alternating fluorene copolymer **1** with a vitrified chiral nematic order have been investigated covering linear dichroism in transmission and reflection, circular differential reflection and transmission as well as optical rotation. All optical signatures are consistent with a left-handed cholesteric organization with a pitch length around 600 nm. In contrast to common belief, we find that even films with thickness an order of magnitude smaller than the pitch length of the cholesteric arrangement show preferential reflection of one of the circular polarizations of light.

## AUTHOR INFORMATION

### Corresponding Author

\*E-mail: [s.c.j.meskers@tue.nl](mailto:s.c.j.meskers@tue.nl); Phone: +31-40-247-3723.

### ORCID

Chidambar Kulkarni: [0000-0001-8342-9256](https://orcid.org/0000-0001-8342-9256)

Daniele Di Nuzzo: [0000-0002-4462-9068](https://orcid.org/0000-0002-4462-9068)

E.W. Meijer: [0000-0003-4126-7492](https://orcid.org/0000-0003-4126-7492)

Stefan C.J. Meskers: [0000-0001-9236-591X](https://orcid.org/0000-0001-9236-591X)

### Notes

The authors declare no competing financial interest.

## ACKNOWLEDGMENTS

We gratefully acknowledge the financial support received from the Dutch Ministry of Education, Culture and Science (Gravity Program No. 024.001.035). C.K. thanks financial support from Marie Skłodowska-Curie (704830) postdoctoral fellowship. D.D.N. acknowledges financial support from the Engineering and Physical Sciences Research Council of the UK (EPSRC).

## REFERENCES

- (1) De Gennes, P. G. *The Physics of Liquid Crystals*; Clarendon Press: Oxford U.K, 1974.
- (2) Wei, S. K. H.; Chen, S. H.; Dolgaleva, K.; Lukishova, S. G.; Boyd, R. W. Robust Organic Lasers Comprising Glassy-Cholesteric Pentafluorene Doped with a Red-Emitting Oligofluorene. *Appl. Phys. Lett.* **2009**, *94*, 041111.
- (3) Halls, J. J. M.; Arias, A. C.; MacKenzie, J. D.; Wu, W. S.; Inbasekaran, M.; Woo, E. P.; Friend, R. H. Photodiodes Based on Polyfluorene Composites: Influence of Morphology. *Adv. Mater.* **2000**, *12*, 498–502.
- (4) Inganäs, O.; Zhang, F.; Andersson, M. R. Alternating Polyfluorenes Collect Solar Light in Polymer Photovoltaics. *Acc. Chem. Res.* **2009**, *42*, 1731–1739.
- (5) Abbel, R.; Schenning, A. P. H. J.; Meijer, E. W. Molecular Weight Optimum in the Mesoscopic Order of Chiral Fluorene (Co)polymer Films. *Macromolecules* **2008**, *41*, 7497–7504.
- (6) Cho, M. J.; Ahn, J.-S.; Kim, Y.-U.; Um, H. A.; Prasad, P. N.; Lee, G. J.; Choi, D. H. New Fluorene-Based Chiral Copolymers with Unusually High Optical Activity in Pristine and Annealed Thin Films. *RSC Adv.* **2016**, *6*, 23879–23886.
- (7) Oh, H. S.; Liu, S.; Jee, H.; Baev, A.; Swihart, M. T.; Prasad, P. N. Chiral Poly(fluorene-alt-benzothiadiazole) (PFBT) and Nanocomposites with Gold Nanoparticles: Plasmonically and Structurally Enhanced Chirality. *J. Am. Chem. Soc.* **2010**, *132*, 17346–17348.
- (8) Grell, M.; Bradley, D. D. C.; Inbasekaran, M.; Woo, E. P. Glass-Forming Conjugated Main-Chain Liquid Crystal Polymer for Polarized Electroluminescence Applications. *Adv. Mater.* **1997**, *9*, 798–802.
- (9) Scherf, U.; Neher, D. Polyfluorenes. *Adv. Polym. Sci.* **2008**, *212*, 1–318.
- (10) Oda, M.; Nothofer, H. G.; Lieser, G.; Scherf, U.; Meskers, S. C. J.; Neher, D. Circularly Polarized Electroluminescence from Liquid-Crystalline Chiral Polyfluorenes. *Adv. Mater.* **2000**, *12*, 362–365.
- (11) Lee, G. J.; Choi, E. H.; Ham, W. K.; Hwangbo, C. K.; Cho, M. J.; Choi, D. H. Circular Dichroism, Surface-Enhanced Raman Scattering, and Spectroscopic Ellipsometry Studies of Chiral Polyfluorene-Phenylene Films. *Opt. Mater. Express* **2016**, *6*, 767–781.
- (12) Lee, D.-M.; Song, J.-W.; Lee, Y.-J.; Yu, C.-J.; Kim, J.-H. Control of Circularly Polarized Electroluminescence in Induced Twist Structure of Conjugate Polymer. *Adv. Mater.* **2017**, *29*, 1700907.
- (13) Lakhwani, G.; Meskers, S. C. J. Circular Selective Reflection of Light Proving Cholesteric Ordering in Thin Layers of Chiral Fluorene Polymers. *J. Phys. Chem. Lett.* **2011**, *2*, 1497–1501.
- (14) Wilson, J. N.; Steffen, W.; McKenzie, T. G.; Lieser, G.; Oda, M.; Neher, D.; Bunz, U. H. F. Chiroptical Properties of Poly(*p*-Phenyleneethynylene) Copolymers in Thin Films: Large *g*-Values. *J. Am. Chem. Soc.* **2002**, *124*, 6830–6831.
- (15) San Jose, B. A.; Matsushita, S.; Akagi, K. Lyotropic Chiral Nematic Liquid Crystalline Aliphatic Conjugated Polymers based on Disubstituted Polyacetylene Derivatives that Exhibit High Dissymmetry Factors in Circularly Polarized Luminescence. *J. Am. Chem. Soc.* **2012**, *134*, 19795–19807.
- (16) Yang, Y.; Correa da Costa, R.; Smilgies, D.-M.; Campbell, A. J.; Fuchter, M. J. Induction of Circularly Polarized Electroluminescence from an Achiral Light-Emitting Polymer via a Chiral Small-Molecule Dopant. *Adv. Mater.* **2013**, *25*, 2624–2628.
- (17) Yan, J.-C.; Cheng, X.; Zhou, Q.-L.; Pei, J. Chiral Polyfluorene Derivatives: Synthesis, Chiroptical Properties, and Investigation of the Structure-Property Relationships. *Macromolecules* **2007**, *40*, 832–839.
- (18) Geng, Y. H.; Trajkovska, A.; Culligan, S. W.; Ou, J. J.; Chen, H. M. P.; Katsis, D.; Chen, S. H. Origin of Strong Chiroptical Activities in Films of Nonfluorenes with a Varying Extent of Pendant Chirality. *J. Am. Chem. Soc.* **2003**, *125*, 14032–14038.
- (19) Bracher, C.; Yi, H.; Scarratt, N. W.; Masters, R.; Pearson, A. J.; Rodenburg, C.; Iraqi, A.; Lidzey, D. G. The Effect of Residual Palladium Catalyst on the Performance and Stability of PCDTBT:PC70BM Organic Solar Cells. *Org. Electron.* **2015**, *27*, 266–273.
- (20) Patel, D.; Graham, K. R.; Reynolds, J. R. A Diels–Alder Crosslinkable Host Polymer for Improved PLED Performance: the Impact on Solution Processed Doped Device and Multilayer Device Performance. *J. Mater. Chem.* **2012**, *22*, 3004–3014.
- (21) Di Nuzzo, D.; Kulkarni, C.; Zhao, B.; Smolinsky, E.; Tassinari, F.; Meskers, S. C. J.; Naaman, R.; Meijer, E. W.; Friend, R. F. High Circular Polarization of Electro-Luminescence Achieved via Self-Assembly of a Light-Emitting Chiral Conjugated Polymer into Multi-Domain Cholesteric Films. *ACS Nano* DOI: [10.1021/acs.nano.7b07390](https://doi.org/10.1021/acs.nano.7b07390).
- (22) Lakhwani, G.; Meskers, S. C. J.; Janssen, R. A. J. Circular Differential Scattering of Light in Films of Chiral Polyfluorene. *J. Phys. Chem. B* **2007**, *111*, 5124–5131.
- (23) Justino, L. L. G.; Ramos, M. L.; Abreu, P. E.; Charas, A.; Morgado, J.; Scherf, U.; Minaev, B. F.; Ågren, H.; Burrows, H. D. Structural and Electronic Properties of Poly(9,9-dialkylfluorene)-Based Alternating Copolymers in Solution: An NMR Spectroscopy and Density Functional Theory Study. *J. Phys. Chem. C* **2013**, *117*, 17969–17982.
- (24) Baessler, H.; Labes, M. M. Determination of the Pitch of a Cholesteric Liquid Crystal by Infrared Transmission Measurements. *Mol. Cryst.* **1969**, *6*, 419–422.
- (25) Dudley, R. J.; Mason, S. F.; Peacock, R. D. Electronic and Vibrational Linear and Circular Dichroism of Nematic and Cholesteric Systems. *J. Chem. Soc., Faraday Trans. 2* **1975**, *71*, 997–1007.
- (26) Spada, G. P.; Brigidi, P.; Gottarelli, G. The Determination of the Handedness of Cholesteric Superhelices Formed by DNA Fragments. *J. Chem. Soc., Chem. Commun.* **1988**, 953–954.
- (27) Maugin, Ch. Sur les Cristaux Liquides de Lehman. *Bull. Soc. Franc. Miner* **1911**, *34*, 71–117.
- (28) Oseen, C. W. The Theory of Liquid Crystals. *Trans. Faraday Soc.* **1933**, *29*, 883–889.

- (29) DeVries, H. L. Rotatory Power and Other Optical Properties of Certain Liquid Crystals. *Acta Crystallogr.* **1951**, *4*, 219–226.
- (30) Belyakov, V. A. *Diffraction Optics of Complex-Structured Periodic Media*; Springer Verlag: Berlin, Germany, 1992.
- (31) Good, R. H.; Karali, A. Transmission of Light Through a Slab of Cholesteric Liquid Crystal. *J. Opt. Soc. Am. A* **1994**, *11*, 2145–2155.
- (32) In an earlier study, see ref 13, we used eq 10 to make an estimate of the pitch in annealed films of **1**. Because eq 10 turns out to be not generally applicable, this estimate is wrong.
- (33) Zhao, Y.; Abdul Rahim, N. A.; Xia, Y.; Fujiki, M.; Song, B.; Zhang, Z.; Zhang, W.; Zhu, X. Supramolecular Chirality in Achiral Polyfluorene: Chiral Gelation, Memory of Chirality, and Chiral Sensing Property. *Macromolecules* **2016**, *49*, 3214–3221.
- (34) Kawagoe, Y.; Fujiki, M.; Nakano, Y. Limonene Magic: Noncovalent Molecular Chirality Transfer Leading to Ambidextrous Circularly Polarised Luminescent  $\pi$ -Conjugated Polymers. *New J. Chem.* **2010**, *34*, 637–647.
- (35) Watanabe, K.; Akagi, K. Helically Assembled  $\pi$ -Conjugated Polymers with Circularly Polarized Luminescence. *Sci. Technol. Adv. Mater.* **2014**, *15*, 044203.
- (36) Fujiki, M. Optically Active Polysilylenes: State-of-the-Art Chiroptical Polymers. *Macromol. Rapid Commun.* **2001**, *22*, 539–563.
- (37) Borrmann, G. Über Extinktionsdiagramme der Röntgenstrahlen von Quarz. *Physik Z.* **1941**, *42*, 157–162.
- (38) Novikov, V. B.; Murzina, T. V. Borrmann Effect in Photonic Crystals. *Opt. Lett.* **2017**, *42*, 1389–1392.
- (39) Chandrasekhar, S. *Liquid Crystals*; Cambridge University Press: Cambridge, U.K., 1992.
- (40) Suresh, K. A. An Experimental Study of the Anomalous Transmission (Borrmann Effect) in Absorbing Cholesteric Liquid Crystals. *Mol. Cryst. Liq. Cryst.* **1976**, *35*, 267–273.